

A deterministic model for non-monotone relationship between translation of upstream and downstream open reading frames

D. E. ANDREEV

*Moscow State University, Moscow, Russia;
Shemyakin-Ovchinnikov Institute of Bioorganic Chemistry, RAS, Moscow, Russia*

P. V. BARANOV

*University College Cork, Cork, Ireland;
Shemyakin-Ovchinnikov Institute of Bioorganic Chemistry, RAS, Moscow, Russia*

A. MILOGORODSKII* AND D. RACHINSKII

University of Texas at Dallas, Richardson, TX, USA

* Corresponding author. Email: axm170052@utdallas.edu

[Received on 28 December 2020]

TASEP modeling was shown to offer a parsimonious explanation for the experimentally confirmed ability of a single upstream Open Reading Frames (uORFs) to upregulate downstream translation during the integrated stress response. As revealed by numerical simulations, the model predicts that reducing the density of scanning ribosomes upstream of certain uORFs increases the flow of ribosomes downstream. To gain a better insight into the mechanism which ensures the non-monotone relation between the upstream and downstream flows, in this work, we propose a phenomenological deterministic model approximating the TASEP model of the translation process. We establish the existence of a stationary solution featuring the decreasing density along the uORF for the deterministic model. Further, we find an explicit non-monotone relation between the upstream ribosome density and the downstream flow for the stationary solution in the limit of increasing uORF length and increasingly leaky initiation. The stationary distribution of the TASEP model, the stationary solution of the deterministic model and the explicit limit are compared numerically.

Keywords: mRNA translation regulation, stress resistance, ordinary differential equation model, asymptotics of stationary solution, modified TASEP model.

1. Introduction

In eukaryotes, canonical translation initiation begins with the recognition of the m7G cap structure found at the 5' end of mRNAs. This is followed by forming the preinitiation complex (PIC), which starts to “scan” the mRNA, unwinding mRNA secondary structures and probing mRNA for potential sites of translation initiation. After the initiation codon is recognized, the chain of events leads to large ribosome subunit joining and initiation of polypeptide synthesis (for more details see recent reviews (Hinnebusch *et al.*, 2016; Hinnebusch, 2014; Asano, 2014; Topisirovic *et al.*, 2011; Jackson *et al.*, 2010) on the mechanism of translation initiation in eukaryotes and its regulation). Once the ribosomes initiate translation, they continue moving along mRNA elongating the peptide chain (elongating ribosomes).

Not all translation initiation events lead to the synthesis of annotated functional proteins. Many codons recognized as starts of translation occur upstream of the annotated coding open reading frame (acORF), which encodes functional proteins in eukaryotic organisms (Pueyo *et al.*, 2016; Johnstone *et al.*,

2016; Wethmar, 2014; von Arnim *et al.*, 2014; Barbosa *et al.*, 2013; Somers *et al.*, 2013; Vilela *et al.*, 2003). Abundant translation initiation upstream of acORFs has been confirmed by several ribosome profiling experiments (Fritsch *et al.*, 2012; Ingolia *et al.*, 2011; Lee *et al.*, 2012). Such translation of an upstream open reading frame (uORF) can regulate eukaryotic gene expression. In particular, ribosome profiling revealed that translation of uORFs is altered in response to changes in physiological conditions.

A number of stress conditions lead to a global increase in translation of uORFs on mRNA leaders (Andreev *et al.*, 2015; Shalgi *et al.*, 2013; Gerashchenko *et al.*, 2012; Ingolia *et al.*, 2009), and sometimes reciprocal changes in acORF translation can be observed among individual mRNAs (Andreev *et al.*, 2015). One of the stress conditions where uORF-mediated translation control seems to be particularly important is in the integrated stress response (ISR) (Andreev *et al.*, 2015; Starck *et al.*, 2016; Young *et al.*, 2016). During ISR the global translation is often down-regulated. This is achieved via molecular events that limit an important initiation factor required for PIC formation, leading to the reduced level of scanning ribosomes at mRNA. However, translation of a small number of mRNAs is resistant to, or upregulated, during ISR, and the most stress resistant mRNAs possess translated uORFs (Andreev *et al.*, 2015; Sidrauski *et al.*, 2015).

The classical mechanism of uORF mediated stress resistance, known as delayed reinitiation, involves several uORFs, and at least two are absolutely essential for stress resistance (Gunisova *et al.*, 2016, 2014; Dever *et al.*, 1992). The archetypical example of this mechanism occurring in yeast has been characterized in details (reviewed in (Hinnebusch, 1993)). On the other hand, examples have been found where only a single uORF is sufficient for imbuing an mRNA with translational stress resistance (Andreev *et al.*, 2015; Palam *et al.*, 2011; Chen *et al.*, 2010; Lee *et al.*, 2009; Zach *et al.*, 2014), suggesting that there are other mechanisms of upregulating gene expression during stress. For instance, the start codon of the uORF is in a suboptimal Kozak context and allows for leaky scanning (Palam *et al.*, 2011; Young *et al.*, 2016) when only part of the ribosomes are initiated at the uORF start codon, while the others bypass it and begin translation at the start codon of the acORF. It has been hypothesized that the stringency of start codon recognition is increased during particular stress conditions, which allows for more leaky scanning, effectively increasing the flow of scanning ribosomes through the uORF and upregulating translation of the acORF (Palam *et al.*, 2011; Young *et al.*, 2016).

It is also possible that elongating ribosomes translating the uORF obstruct progression of scanning ribosomes downstream, and this obstruction is relieved during stress due to reduced number of elongating ribosomes (albeit the stringency of the start codon recognition remains unchanged). In this scenario, the intensities of the flows of scanning ribosomes upstream and downstream the uORF are negatively correlated due to the obstruction of scanning ribosomes, which may potentially explain how a single uORF mediates stress resistance. However, it is *a priori* unclear whether such a mechanism is plausible without additional factors involved because stress reduces the number of both elongating and scanning ribosomes creating counteracting tendencies. While most stress resistant mRNAs possess uORFs, only very few uORF-containing mRNAs are stress resistant (Andreev *et al.*, 2015). This leads to the question what makes some uORFs to be the providers of stress resistance? In particular, can the interaction of scanning and elongating ribosomes trailing along the uORF explain the upregulation of downstream expression during stress?

The latter question was recently explored using a variant of the Totally Asymmetric Simple Exclusion Process (TASEP) model (Andreev *et al.*, 2018). Computer simulations of the model predicted that indeed a small subset of specific uORFs (constrained by length and leakiness of their initiation sites) are capable of upregulating translation downstream of a single uORF in response to the reduced availability of ribosomes upstream, which is observed under ISR.

TASEP is a stochastic dynamical system of unidirectional particle movement through a one dimen-

sional lattice, where each site can be occupied by no more than one particle, and the probability of particle transition from one site to another is predefined. Beginning with (MacDonald *et al.*, 1968), it has provided a basis for most mechanistic studies of mRNA translation dynamics and has been widely used for modeling a variety of dynamical systems including non-equilibrium transport phenomena, biological systems and road traffic (Ciandrini *et al.*, 2010; Grüne *et al.*, 2020; Reuveni *et al.*, 2011; von der Haar, 2012; Zhao *et al.*, 2014; Zia *et al.*, 2011; Zur *et al.*, 2016; Gorban *et al.*, 2012). In the classical setting, the number of particles is conserved. In this case, important mathematical tools for the analysis of the stationary distribution of the TASEP model with the associated phase transitions are provided by the so-called hydrodynamic limit, which takes the form of a parabolic differential equation (for the density of the particles) expressing the conservation law (Derrida *et al.*, 1997; Blythe *et al.*, 2007). The hydrodynamic limit has been recently extended to a generalized version of the TASEP model (the ℓ -TASEP with particles occupying multiple sites on the lattice and inhomogeneous jump rates), which was applied to analyze mRNA translation efficiency (Schönherr *et al.*, 2004; Erdmann-Pham *et al.*, 2020).

The variant of the ℓ -TASEP model developed in (Andreev *et al.*, 2018) was based on the assumption that collisions of elongating ribosomes with scanning ribosomes can result in the dissociation of the latter from the mRNA. Hence, the conservation is violated. In this work, we propose a deterministic model of the uORF-mediated stress resistance based on a similar set of assumptions and additional simplifications. This system is less flexible than the probabilistic non-conservative ℓ -TASEP model, which for example can account for the fact that ribosomes occupy multiple sites on mRNA (Andreev *et al.*, 2018). On the other hand, the added value of the deterministic model is that it lends itself to rigorous analysis and admits an explicit solution in limit cases, providing further insight into a plausible mechanism of uORF-mediated stress resistance. Using this deterministic model, we confirm that leaky initiation combined with removal of scanning ribosomes due to collisions with elongating ribosomes can explain the non-monotone relationship between the flows of scanning ribosomes upstream and downstream of the uORF.

The deterministic model relates the rate of change of the average densities of scanning and elongating ribosomes at each mRNA site, ρ_n^s and ρ_n^e , respectively, to the densities at neighboring sites. As described in Section 2, it is assumed that the flow of scanning ribosomes from site n to the next site is proportional to the product of the density ρ_n^s and the probability $1 - \rho_{n+1}^s - \rho_{n+1}^e$ that the next site is unoccupied. The exit flow of scanning ribosomes from each site n is assumed proportional to the product of the density ρ_n^s and the density ρ_{n-1}^e of elongating ribosomes at the previous site.

The paper is organized as follows. The next section presents the stochastic TASEP model and the deterministic model of uORF translation. Section 3 contains main results. We show that the deterministic model has a stationary solution with certain properties and find this solution in the limit of increasing mRNA length. This allows us to infer conditions that ensure the non-monotone dependence of the downstream flow on the upstream flow of scanning ribosomes. In Section 4, we compare numerically the predictions of the TASEP and deterministic models with the explicit limit solution. Section 5 contains the proofs.

2. Models

2.1 Modified TASEP model for propagation of ribosomes along uORF

We represent scanning and elongating ribosomes as two separate types of particles with different dynamic properties with the possibility of transformation of one into the other at specific sites. The uORF is modeled as a discrete array of positions numbered from 0 to N . Each position represents one codon. Position N_1 corresponds to the start codon, position $N_1 + N_2$ corresponds to the stop codon. Particles

of the first kind (representing scanning ribosomes) proceed from position 0 to position N_1 , where part of them is converted to particles of the second kind (representing elongating ribosomes), see Figure 1. Then, particles of both kinds proceed to the position $N_1 + N_2$, where particles of the second kind are eliminated. Particles of the first kind continue to the position $N_* - 1$ and are eliminated there. Hence, particles of the second kind can be encountered between the positions N_1 and $N_1 + N_2$ only.

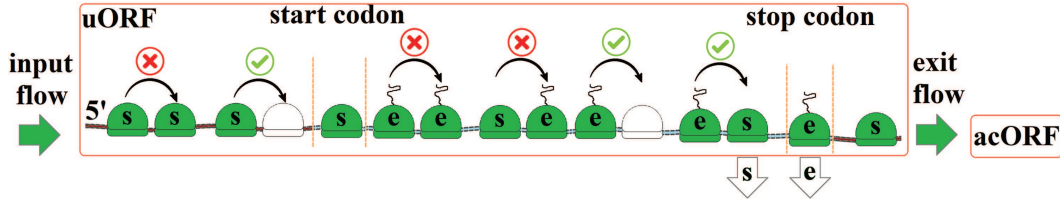


FIG. 1. Block scheme of the TASEP model of the uORF translation.

As the first model, we consider a modification of the TASEP stochastic process. The state of the model at time $k \in \mathbb{N}_0$ is a vector $s^k = (s_0^k, \dots, s_{N_*-1}^k)$ with $s_i^k \in \{0, 1, 2\}$, where $s_i^k = 0$ corresponds to the vacant (unoccupied) codon, $s_i^k = 1$ corresponds to the codon occupied by a particle of the first kind and $s_i^k = 2$ corresponds to the codon occupied by a particle of the second kind at the position i . At every time step, a position $n = n_k$ is selected at random with equal probability $1/N_*$. If either $s_{n_k}^k \neq 0$ or $n_k = 0$, then the components $s_{n_k}^k$ and $s_{n_k+1}^k$ of the state are changed according to the rules listed in Table 1 (in the case $n_k = N_* - 1$, only $s_{N_*-1}^k$ is changed). The other components remain unchanged, i.e. $s_m^{k+1} = s_m^k$ for $m \neq n_k, n_k + 1$.

In the cases, which are not listed in Table 1, the state remains unchanged. In particular, $s^{k+1} = s^k$ if either $s_{n_k}^k = 0$ for $n_k \neq 0$ or $(s_{n_k}^k, s_{n_k+1}^k) \in \{(1, 1), (1, 2), (2, 2)\}$.

Table 1. Probabilities of transitions $(s_{n_k}^k, s_{n_k+1}^k) \rightarrow (s_{n_k}^{k+1}, s_{n_k+1}^{k+1})$

$n_k \neq 0, N_1 - 1, N_1 + N_2 - 1, N_* - 1$:	$(1, 0) \rightarrow (0, 1)$ with probability 1; $(2, 0) \rightarrow (0, 2)$ with probability 1; $(2, 1) \rightarrow (0, 2)$ with probability 1;
$n_k = 0$:	$(0, 0) \rightarrow (1, 0)$ with probability $\rho^0 \in (0, 1]$; $(0, 1) \rightarrow (0, 1)$ with probability $1 - \rho^0$; $(1, 0) \rightarrow (1, 1)$ with probability ρ^0 ; $(1, 0) \rightarrow (0, 1)$ with probability $1 - \rho^0$;
$n_k = N_1 - 1$:	$(1, 0) \rightarrow (0, 2)$ with probability $c \in (0, 1)$; $(1, 0) \rightarrow (0, 1)$ with probability $1 - c$;
$n_k = N_1 + N_2 - 1$:	$(1, 0) \rightarrow (0, 1)$ with probability 1; $(2, 0) \rightarrow (0, 0)$ with probability 1; $(2, 1) \rightarrow (0, 1)$ with probability 1;
$n_k = N_* - 1$:	$s_{N_*-1}^k = 1 \rightarrow s_{N_*-1}^{k+1} = 0$ with probability 1.

These rules imply that a particle of the first kind, if selected at a particular time step, moves from its position n_k to the next position $n_k + 1$ provided that the latter is vacant. A particle of the second kind moves to the next position if this position is either vacant or occupied by a particle of the first kind. In the latter case, the particle of the second kind replaces the particle of the first kind eliminating it from the array. Special rules apply for $n_k = 0, N_1 - 1, N_1 + N_2 - 1, N_* - 1$. The initial position $n = 0$, if vacant, is refilled by a particle of the first kind with the probability ρ^0 . A particle of the first kind is converted into a particle of the second kind with the probability c when moved from the position $N_1 - 1$ to N_1 . Particles of the second kind are eliminated at the position $N_1 + N_2 - 1$, and particles of the second kind are removed at the position $N_* - 1$. The model is initiated with the state $s^0 = (1, 0, \dots, 0)$.

Results of numerical simulation of this model are presented in Section 4.

2.2 Deterministic model

Now, we consider a phenomenological deterministic model, which approximates the above stochastic process.

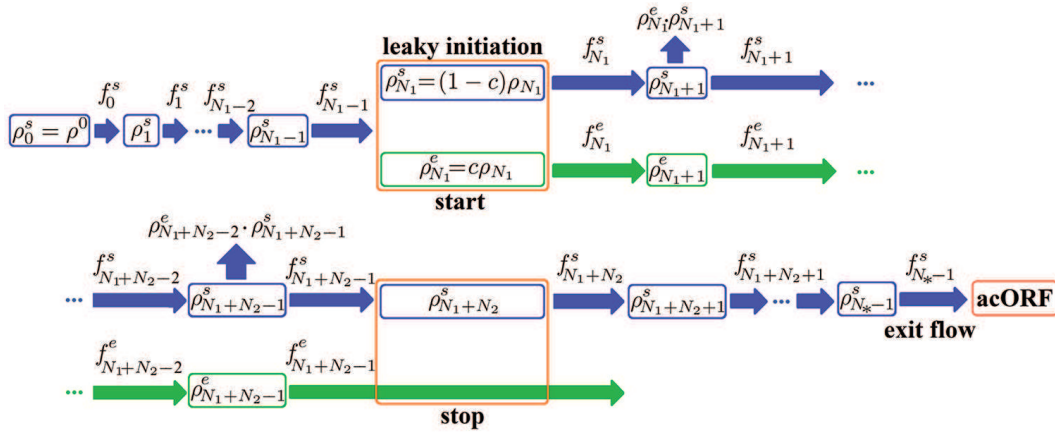


FIG. 2. Block scheme of the deterministic model of the uORF translation.

By ρ_n^s and ρ_n^e we denote the densities of particles of the first and second kind, respectively, at position n . These densities satisfy $0 \leq \rho_n^s, \rho_n^e \leq \rho_n^s + \rho_n^e \leq 1$. The boundary conditions for particles of the first kind are

$$\rho_0^s = \rho^0, \quad \rho_{N_*}^s = 0. \quad (2.1)$$

Since there are no particles of the second kind outside the segment between the start and stop codons, we require

$$\rho_0^e = \rho_1^e = \dots = \rho_{N_1-1}^e = \rho_{N_1+N_2}^e = \rho_{N_1+N_2+1}^e = \dots = \rho_{N_*}^e = 0. \quad (2.2)$$

It is postulated that the one-directional flow of particles of the first kind from position n to position $n + 1$ equals

$$f_n^s = \rho_n^s(1 - \rho_{n+1}^s - \rho_{n+1}^e), \quad n = 0, 1, \dots, N_* - 1;$$

the flow of particles of the second kind from position n to position $n + 1$ is

$$f_n^e = \rho_n^e(1 - \rho_{n+1}^e), \quad n = 0, 1, \dots, N_* - 1.$$

Using these formulas for the flows, the balance equation for particles of the first kind at any position $n \neq N_1$ reads

$$\frac{1}{v} \dot{\rho}_n^s = f_{n-1}^s - f_n^s - \rho_n^s \rho_{n-1}^e, \quad n = 1, \dots, N_* - 1; \quad n \neq N_1, \quad (2.3)$$

where v is the velocity of the particles, and the last term, $-\rho_n^s \rho_{n-1}^e$, accounts for collisions of particles of the second kind with particles of the first kind. It is assumed that such a collision results in the elimination of the particle of the first kind. The balance equations for particles of the second kind for n between the start and the stop codon are

$$\frac{1}{v} \dot{\rho}_n^e = f_{n-1}^e - f_n^e, \quad n = N_1 + 1, \dots, N_1 + N_2 - 1. \quad (2.4)$$

At $n = N_1$ (the start codon), the balance equation is slightly different:

$$\dot{\rho}_{N_1} = f_{N_1-1}^s - f_{N_1}^s - f_{N_1}^e, \quad (2.5)$$

where $\rho_{N_1} = \rho_{N_1}^s + \rho_{N_1}^e$ is the total density of particles at the start codon.

Balance equations (2.3)–(2.5) and boundary conditions (2.1)–(2.2) are coupled with the matching conditions at the start codon:

$$\rho_{N_1}^s = (1 - c) \rho_{N_1}, \quad \rho_{N_1}^e = c \rho_{N_1}, \quad (2.6)$$

where the parameter $c \in (0, 1)$ determines the fraction of particles of the first kind converted to particles of the second kind at the start codon.

3. Main results

3.1 Existence of a stationary solution

We consider the stationary solution of problem (2.1)–(2.6). For this solution the flow of particles of the first kind is constant on the segments $0 \leq n \leq N_1 - 1$ and $N_1 + N_2 \leq n \leq N_* - 1$ and the flow of particles of the second kind is constant between the start and stop codons:

$$f_0^s = \dots = f_{N_1-1}^s = j^{(1)}; \quad f_{N_1}^e = \dots = f_{N_1+N_2-1}^e = J^{(2)}; \quad (3.1)$$

$$f_{N_1+N_2}^s = \dots = f_{N-1}^s = j^{(3)}. \quad (3.2)$$

It will be convenient to slightly change the notation and denote

$$\rho_n^{(1)} = \rho_n^s, \quad n = 0, \dots, N_1 - 1; \quad \rho_{N_1}^{(1)} = \rho_{N_1};$$

$$\rho_m^{(2)} = \rho_{N_1+m}^s, \quad R_m = \rho_{N_1+m}^e, \quad m = 0, \dots, N_2 + N_3,$$

where $N_3 = N_* - N_1 - N_2$, as well as to introduce the new variables

$$j_m^{(2)} = \rho_m^{(2)} (1 - \rho_m^{(2)}), \quad m = 0, \dots, N_2 + N_3 - 1.$$

That is, $\rho_n^{(1)}$ are densities of particles of the first kind upstream of the start codon, $\rho_m^{(2)}$ are densities of particles of the first kind downstream of the start codon and R_m are densities of particles of the second kind downstream of the start codon. Note that $j_m^{(2)}$ is not equal to the flow $f_{N_1+m}^s$.

With this notation, the stationary solution satisfies the system of equations

$$\rho_{n+1}^{(1)} = 1 - \frac{j^{(1)}}{\rho_n^{(1)}}, \quad n = 0, \dots, N_1 - 1; \quad (3.3)$$

$$R_{m+1} = \begin{cases} 1 - \frac{j^{(2)}}{R_m}, & m = 0, \dots, N_2 - 1; \\ R_m, & m = N_2, \dots, N_2 + N_3 - 1; \end{cases} \quad (3.4)$$

$$\begin{cases} \rho_{m+1}^{(2)} = 1 - \frac{j_m^{(2)}}{\rho_m^{(2)}}, & m = 0, \dots, N_2 + N_3 - 1; \\ j_{m+1}^{(2)} = j_m^{(2)} - R_{m+1}\rho_m^{(2)} - (R_m - R_{m+2})\rho_{m+1}^{(2)}, & m = 0, \dots, N_2 + N_3 - 2, \end{cases} \quad (3.5)$$

coupled with the boundary and matching conditions

$$\begin{aligned} \rho_0^{(1)} = \rho^0; \quad R_0 = c\rho_{N_1}^{(1)}; \quad \rho_0^{(2)} = (1-c)\rho_{N_1}^{(1)}; \\ j^{(1)} = j_0^{(2)} + J^{(2)} - \rho_0^{(2)}R_1; \quad R_{N_2} = 0; \quad \rho_{N_2+N_3}^{(2)} = 0. \end{aligned} \quad (3.6)$$

A solution of problem (3.3)–(3.6) is called *positive* if all its unknown components are positive:

$$\rho_0^{(1)}, \dots, \rho_{N_1}^{(1)}; \rho_0^{(2)}, \dots, \rho_{N_2+N_3-1}^{(2)}; R_0, \dots, R_{N_2-1}; j^{(1)}; j_0^{(2)}, \dots, j_{N_2+N_3-1}^{(2)}; J^{(2)} > 0. \quad (3.7)$$

A solution is called *decreasing* if

$$\rho_0^{(1)} > \dots > \rho_{N_1}^{(1)} > \rho_0^{(2)} > \dots > \rho_{N_2+N_3}^{(2)} = 0; \quad R_0 > \dots > R_{N_2} = 0.$$

THEOREM 3.1 Given any $\rho^0 \in (0, 1/2]$, $c \in (0, 1)$, problem (3.3)–(3.6) has a positive decreasing solution.

This theorem is proved in the next section.

3.2 Continuous limit of the stationary solution

Denote by $W : [-e^{-1}, \infty) \rightarrow [-1, \infty)$ the Lambert W -function, which is the inverse of the function $W^{-1}(w) = we^w$. Denote

$$\varphi(\rho) = \rho(1 - \rho), \quad (3.8)$$

$$\rho_*(\rho^0, \tau) = -\frac{1}{2}W\left(-2\rho^0 e^{-\rho^0(2+c_0\tau)}\right). \quad (3.9)$$

Below we use the notation $x_n = O(N_2^\alpha)$ if $|x_n| \leq CN_2^\alpha$, where C is independent of N_2 for a given range of the values of n .

THEOREM 3.2 Suppose that $c = c_0/N_2$ with a constant $c_0 > 0$. Let $0 < \rho^0 < 1/2$. Then, the positive decreasing solution of problem (3.3)–(3.6) satisfies

$$\rho_n^{(1)} = \rho^0 + O(N_2^{-1}), \quad 0 \leq n \leq N_1, \quad (3.10)$$

$$\rho_m^{(2)} = \rho_*\left(\rho^0, \frac{m}{N_2}\right) + O(N_2^{-1}), \quad 0 \leq m \leq N_2 - \frac{\ln N_2}{\ln(1/\rho_0 - 1)}, \quad (3.11)$$

$$j^{(1)} = \varphi(\rho^0) + O(N_2^{-1}), \quad (3.12)$$

$$j_m^{(2)} = \varphi\left(\rho_*\left(\rho^0, \frac{m}{N_2}\right)\right) + O(N_2^{-1} \ln N_2), \quad 0 \leq m \leq N_2, \quad (3.13)$$

$$j^{(3)} = \varphi(\rho_*(\rho^0, 1)) + O(N_2^{-1} \ln N_2) \quad (3.14)$$

as $N_2 \rightarrow \infty$, where the functions φ, ρ_* are defined by (3.8), (3.9).

The proof is presented in the next section.

REMARK 3.1 It is easy to see that the limit exit flow $j_*^{(3)}(\rho^0) = \varphi(\rho_*(\rho^0, 1))$ achieves its maximum over the interval $0 \leq \rho^0 \leq 1/2$ at the point

$$\rho^0 = \frac{1}{2 + c_0}. \quad (3.15)$$

Thus, formula (3.14) of Theorem 3.2 ensures that the exit flow $j^{(3)} = f_{N_*-1}^s$ of scanning ribosomes defined by the stationary solution of model (2.1)–(2.6) reaches a maximum value when the initial density is close the value (3.15) if N_2 is sufficiently large. In other words, the dependence of the exit flow on the initial density of scanning ribosomes is non-monotone.

REMARK 3.2 If N_2 is sufficiently large and $N_3 = 0$ (the uORF ends at the stop codon), then according to Theorem 3.2, the density $\rho_m^{(2)}$ of scanning ribosomes drops from approximately the value $\rho_*(\rho^0, 1) > 0$ to zero over a relatively short segment of the uORF adjacent to its downstream end. In other words, the distribution of the density of scanning ribosomes over uORF has a boundary layer at the downstream end. The relative width of this boundary layer according to Theorem 3.2 is of the order of $N_2^{-1} \ln N_2$.

The situation is similar for $N_3 > 0$. In this case, on the uORF segment downstream of the stop codon the density increments satisfy

$$0 \leq \rho_{m-1}^{(2)} - \rho_m^{(2)} \leq \frac{\rho^0}{1 - \rho^0} (\rho_m^{(2)} - \rho_{m+1}^{(2)}). \quad (3.16)$$

Due to this relationship, for sufficiently large N_3 , the density distribution exhibits one boundary layer, which is located at the downstream end of the uORF.

REMARK 3.3 The biologically relevant situation corresponds to relatively small values of ρ^0 (the low density regime). For completeness, let us discuss larger densities as well.

The continuous limit of the standard TASEP model with the conserved flow undergoes a bifurcation as the density increases. The saturated congestion regime corresponds to all densities exceeding 0.5 and is characterized by the same maximal flow of particles. This applies to the initial segment $0 \leq n \leq N_1$ of the TASEP model described in Section 2.1. Therefore, the exit flow of this model has the same value for all the initial densities $\rho^0 \geq 0.5$. Numerical examples are considered in the next section.

4. Numerical results

Figure 3 shows the dependence of the exit flow $j^{(3)} = j^{(3)}(\rho^0)$ of scanning ribosomes at $n = N_*$ on the initial density ρ^0 at $n = 0$. The function $j^{(3)} = j^{(3)}(\rho^0)$ is obtained from the stationary distribution of the TASEP model and the stationary solution of the approximating deterministic model (2.1)–(2.6).

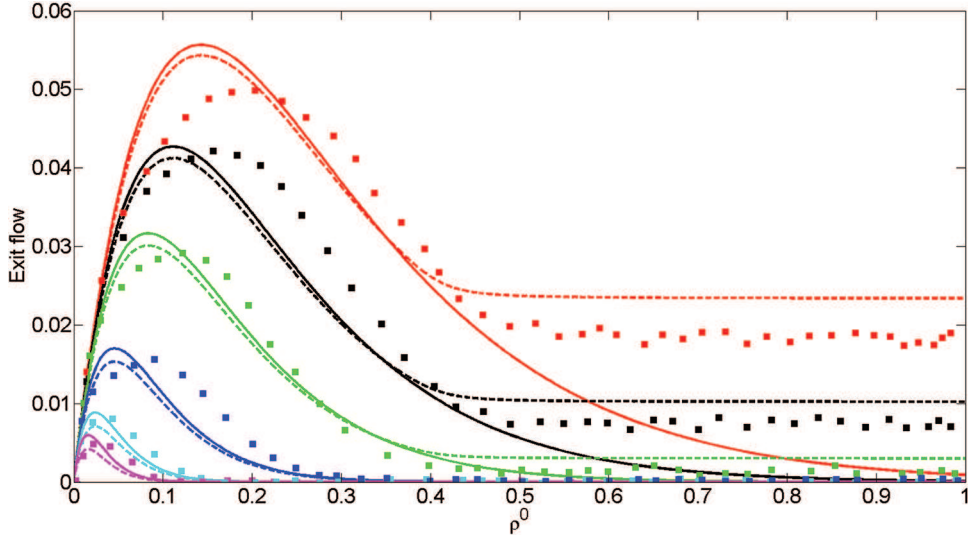


FIG. 3. Exit flow of scanning ribosomes as a function of the density ρ^0 of ribosomes at $n = 0$ for different values of the conversion rate, c , of scanning ribosomes to elongating ribosomes at the start codon. Dots correspond to the stationary distribution of the TASEP model, dashed curves correspond to the stationary solution of the deterministic model (2.1)–(2.6), and solid curves correspond to the explicit formula for the limit exit flow, $j_*^{(3)}(\rho^0) = \varphi(\rho_*(\rho^0, 1))$, of Theorem 3.2 and Remark 3.1. The red, black, green, blue, cyan and pink curves correspond to $c = 0.025, 0.035, 0.05, 0.1, 0.2, 0.3$, respectively; $N_1 = N_3 = 100, N_2 = 200$.

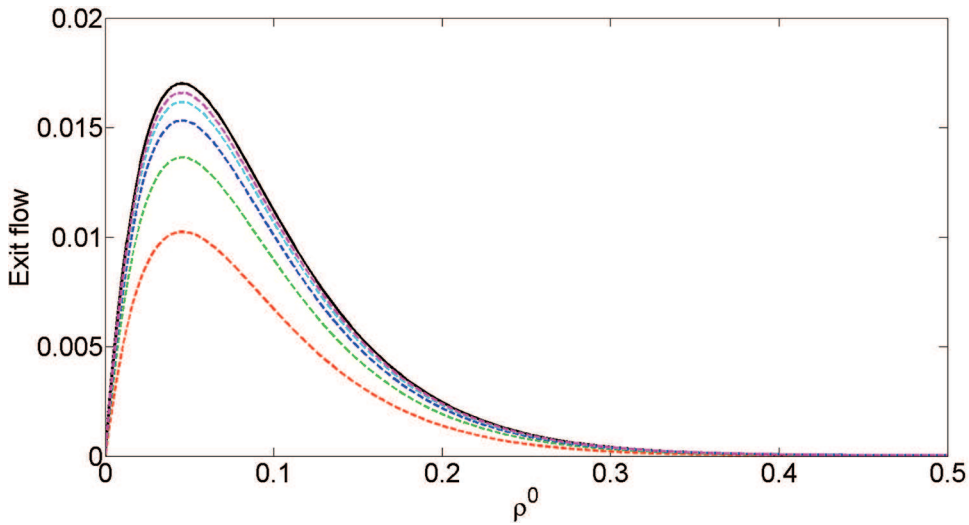


FIG. 4. Exit flow of scanning ribosomes as a function of the density ρ^0 for different length of the uORF. The conversion rate of scanning ribosomes to elongating ribosomes scales with N_2 as $c = c_0/N_2$ where $c_0 = 20$ is fixed, see in Theorem 3.2. The black solid curve corresponds to the explicit formula for the limit exit flow, $j_*^{(3)}(\rho^0) = \varphi(\rho_*(\rho^0, 1))$, see Remark 3.1. The dashed curves are obtained from the stationary solution of the deterministic model (2.1)–(2.6). The pink, cyan, blue, green and red curves correspond to $N_2 = 50, 100, 200, 400, 800$, respectively; $N_1 = N_3 = 100$.

The exit flow peaks between $\rho^0 = 0$ and $\rho^0 = 0.5$. One can see that the peak predicted by the TASEP model is shifted to the right of the peak obtained from the deterministic model, and tends to be wider for the TASEP model. As expected, the output decreases with the increasing rate c of conversion of scanning to elongating ribosomes at the start codon.

In accordance with Theorem 3.2, the dependence of the exit flow on the initial density, $j^{(3)}(\rho^0)$, for the stationary solution of the deterministic model (2.1)–(2.6) is well approximated by the composition $\varphi \circ \rho_*$ of the functions (3.8) and (3.9) on the interval $0 < \rho^0 < 1/2$, see Figures 3 and 4.

According to Remark 3.3, the stationary distribution of the TASEP model features (approximately) the same exit flow of scanning ribosomes for all the initial densities $1/2 \leq \rho^0 < 1$. The same is true for the deterministic model (2.1)–(2.6), see Figure 3.

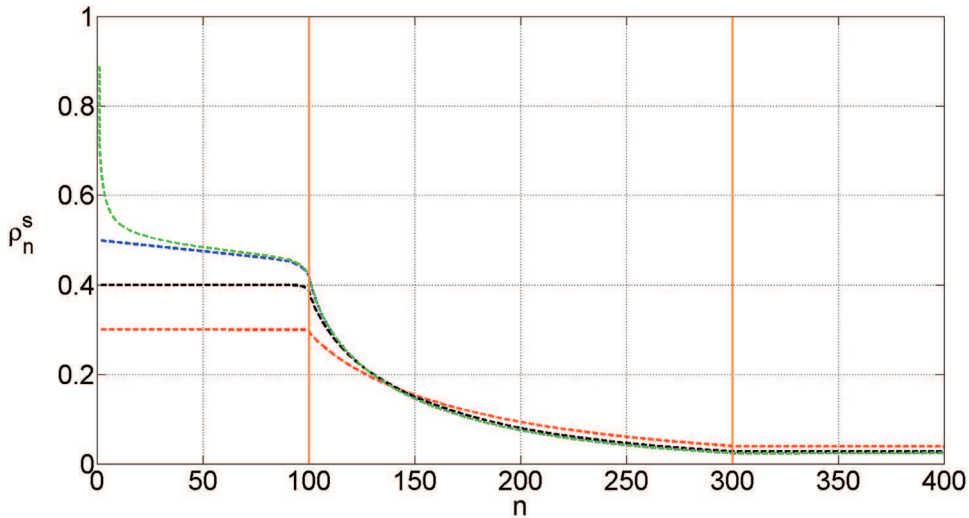


FIG. 5. The dependence of the density ρ_n^s on the position n along the uORF for the stationary solution of the deterministic model (2.1)–(2.6). The red, black, blue and green curves correspond to $\rho^0 = 0.3, 0.4, 0.5, 0.9$, respectively; $N_1 = N_3 = 100, N_2 = 200$; $c = 0.025$. Vertical lines indicate the position of the start and stop codons.

Figures 5 and 6 present the stationary distribution of density and flow of scanning ribosomes, respectively, for the deterministic model (2.1)–(2.6) for different values of the initial density and $N_2 = 200$. On the interval $N_1 \leq n \leq N_1 + N + 2$, each density graph is practically indistinguishable from the limit density curve $\rho_n = \rho_*(\rho^0, n/N_2)$ with the corresponding ρ^0 (not shown). This agrees with Theorem 3.2. Similarly, the flow graphs are very close to the limit curves $f_n = \varphi(\rho_*(\rho^0, n/N_2))$ corresponding to the limit $N_2 \rightarrow \infty$. The flow graphs with $\rho^0 \geq 1/2$ practically coincide with each other (the blue and green curves in Figure 6). The flow reaches its maximum value $1/4$ on the initial segment $0 \leq n \leq N_1$ for $\rho^0 \geq 1/2$. The density graphs with $\rho^0 \geq 1/2$ feature a boundary layer near $n = 0$ and almost coincide with each other for larger values of n (see the plots of the same color in Figure 5).

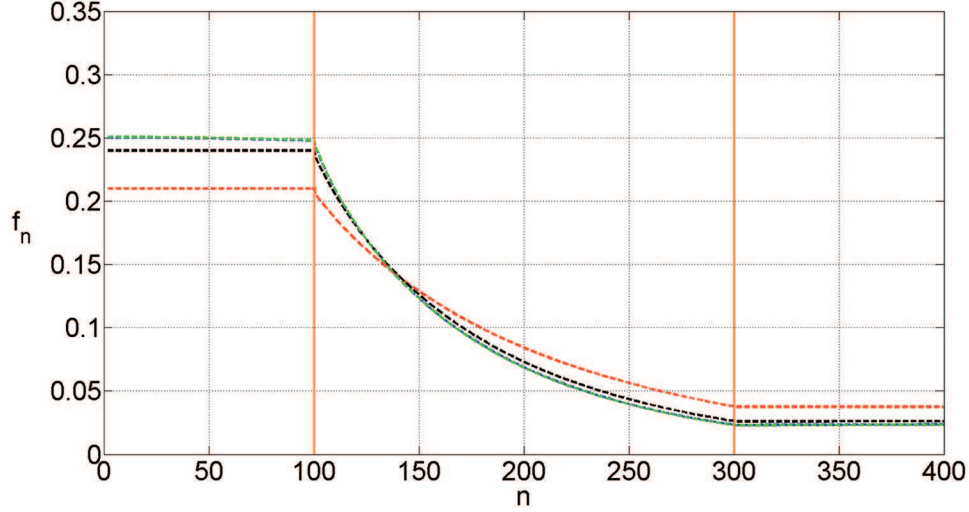


FIG. 6. The dependence of the flow f_n of scanning ribosomes on the position n along the uORF for the stationary solution of the deterministic model (2.1)–(2.6). The color code and density are the same as in Figure 5.

5. Proofs

5.1 Auxiliary lemmas

The proof of Theorem 3.1 uses a few auxiliary lemmas.

Consider iterations

$$\rho_{n+1} = 1 - \frac{j}{\rho_n}, \quad \rho_0 = \rho^0, \quad n = 0, 1, 2, \dots \quad (5.1)$$

Since the sequence (5.1) is defined by j and ρ^0 , we write $\rho_n = \rho_n(j, \rho^0)$. The following lemma summarizes simple properties of this sequence.

LEMMA 5.1 Given an $N \geq 1$, there is a continuous strictly increasing function $\psi_N : [0, 1] \rightarrow \mathbb{R}_+$ satisfying

$$\psi_N(\rho) > \varphi(\rho) = \rho(1 - \rho), \quad 0 \leq \rho \leq 1,$$

and the corresponding domain

$$\mathcal{D}_N = \{(j, \rho^0) : 0 < j < \psi_N(\rho^0), \ 0 < \rho^0 < 1\},$$

such that

- The following relation holds:

$$\rho_N(\psi_N(\rho^0), \rho^0) = 0;$$

- For every $(j, \rho^0) \in \mathcal{D}_N$, the iterations $\rho_n = \rho_n(j, \rho^0)$ defined by (5.1) satisfy

$$\rho_0, \rho_1, \dots, \rho_N > 0;$$

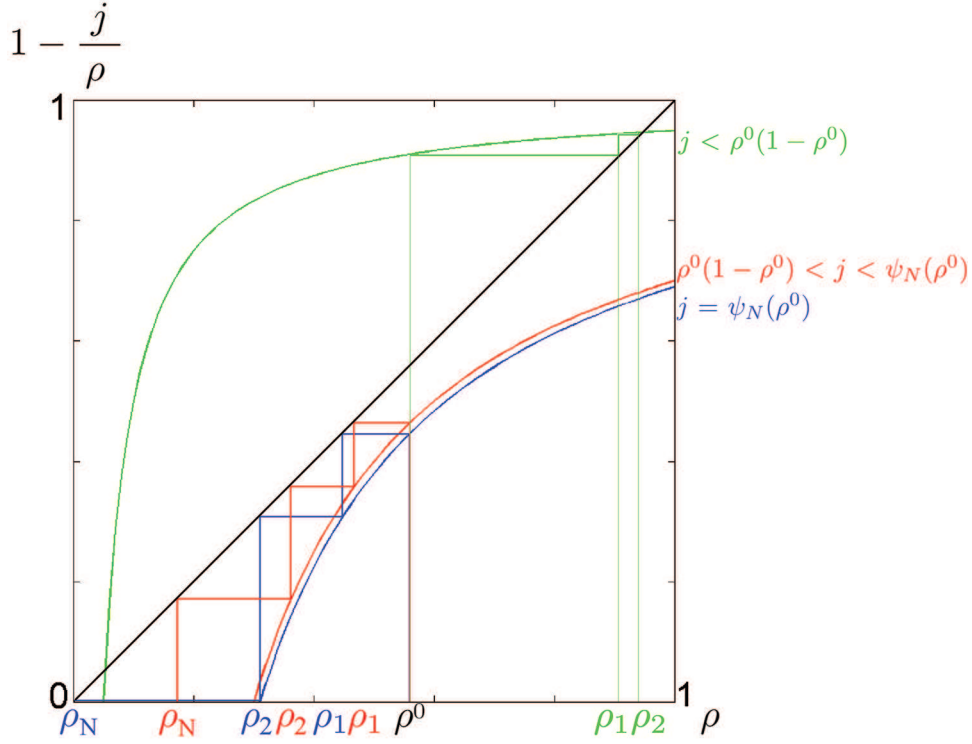


FIG. 7. The cobweb plot of the sequence (5.1) for different values of j . The green, red and blue correspond to $j = 0.05, 0.3, 0.31$, respectively; $\rho^0 = 0.58$.

- The iterations $\rho_0, \rho_1, \dots, \rho_N$ strictly decrease if $j > \rho^0(1 - \rho^0)$, strictly increase if $j < \rho^0(1 - \rho^0)$, and satisfy $\rho_0 = \dots = \rho_N = \rho^0$ if $j = \rho^0(1 - \rho^0)$ for $(j, \rho^0) \in \mathcal{D}_N$;
- The continuous functions $\rho_n = \rho_n(j, \rho^0) : \mathcal{D}_N \rightarrow \mathbb{R}$ strictly decrease in j and strictly increase in ρ^0 for all $1 \leq n \leq N$;
- On the boundary of \mathcal{D}_N ,

$$\rho_N(j, \rho^0) \rightarrow 1 \quad \text{as } j \rightarrow 0+; \quad \rho_{N+1}(j, \rho^0) \rightarrow -\infty \quad \text{as } j \rightarrow \psi_N(\rho^0)-.$$

Proof. The above statement directly follows from the definition of the sequence (5.1), see Figure 7. \square
Two remarks are in order.

REMARK 5.1 Relations

$$\rho_1 = 1 - \frac{j}{\rho^0} > 0 \quad \text{for every } 0 < j < \psi_N(\rho^0)$$

imply

$$\psi_N(\rho) \leq \rho, \quad 0 \leq \rho \leq 1. \quad (5.2)$$

REMARK 5.2 From Lemma 5.1, it follows that iterations (5.1) with $j = \psi_N(\rho^0)$ satisfy

$$j = \psi_N(\rho^0) \quad \Rightarrow \quad \rho_0 > \rho_1 > \cdots > \rho_{N-1} > 0 = \rho_N, \quad (5.3)$$

where each $\rho_n = \rho_n(\psi_N(\rho^0), \rho^0)$, $n = 0, \dots, N-1$, strictly increases with ρ^0 . Moreover, each difference $\rho_{n-1} - \rho_n$ strictly increases with ρ^0 . Indeed, from the relations

$$\rho_n - \rho_{n+1} = \frac{j}{\rho_n} - \frac{j}{\rho_{n-1}} = \frac{j(\rho_{n-1} - \rho_n)}{\rho_{n-1}\rho_n} = \frac{1 - \rho_n}{\rho_n}(\rho_{n-1} - \rho_n) = \left(\frac{1}{\rho_n} - 1\right)(\rho_{n-1} - \rho_n),$$

it follows that

$$\rho_{n-1} - \rho_n = (\rho_{N-1} - \rho_N) \prod_{k=n}^{N-1} \frac{1}{\frac{1}{\rho_k} - 1}.$$

Since $\rho_N = 0$ and all the ρ_n increase with ρ^0 , we see that each difference

$$\rho_{n-1} - \rho_n = \rho_{n-1}(\psi_N(\rho^0), \rho^0) - \rho_n(\psi_N(\rho^0), \rho^0), \quad n = 1, \dots, N, \quad (5.4)$$

increases with ρ^0 .

Now, let us consider the following iterations:

$$\begin{cases} \rho_{n+1} = 1 - \frac{j_n}{\rho_n}, \\ j_{n+1} = j_n - r_n \rho_n - \delta_n \rho_{n+1}, \end{cases} \quad (5.5)$$

where $n = 0, 1, 2, \dots$. In the following lemma, we compare two sequences $\{(j_n, \rho_n)\}$ and $\{(\hat{j}_n, \hat{\rho}_n)\}$, which start from different initial conditions and possibly have different sequences of coefficients $\{r_n\}$, $\{\delta_n\}$ and $\{\hat{r}_n\}$, $\{\hat{\delta}_n\}$, respectively.

LEMMA 5.2 System (5.5) depends monotonically on the sequences $\{r_n\}$, $\{\delta_n\}$ and on the initial conditions in the positive quadrant in the following sense:

If

$$0 \leq \hat{r}_n \leq r_n, \quad 0 \leq \hat{\delta}_n \leq \delta_n, \quad n = 0, \dots, N-1,$$

$$\hat{j}_n, j_n, \hat{\rho}_n, \rho_n > 0, \quad n = 0, \dots, N,$$

and $\hat{j}_0 \geq j_0$, $\hat{\rho}_0 \leq \rho_0$, then

$$\hat{j}_n \geq j_n, \quad \hat{\rho}_n \leq \rho_n, \quad n = 1, \dots, N.$$

Proof. The statement follows directly from (5.5) by induction in n . \square

LEMMA 5.3 Suppose

$$\rho_0^{(2)}, \dots, \rho_k^{(2)} > 0, \quad \rho_k^{(2)} > \rho_{k+1}^{(2)}, \quad j_k^{(2)} > 0. \quad (5.6)$$

Then,

$$\rho_0^{(1)} > \cdots > \rho_{N_1}^{(1)} > \rho_0^{(2)} > \cdots > \rho_k^{(2)} > \rho_{k+1}^{(2)}. \quad (5.7)$$

Proof. By Lemma 5.1, $R_0 > R_1 > \dots > R_{N_2} = 0$. Therefore, the sequence $j_n^{(2)}$ decreases. If $\rho_n^{(2)} \geq \rho_{n-1}^{(2)} > 0$ for some $n \leq k$, then due to $j_{n-1}^{(2)} \geq j_n^{(2)} \geq j_k^{(2)} > 0$,

$$\rho_{n+1}^{(2)} = 1 - \frac{j_n^{(2)}}{\rho_n^{(2)}} \geq 1 - \frac{j_{n-1}^{(2)}}{\rho_{n-1}^{(2)}} = \rho_n^{(2)}.$$

That is, $\rho_n^{(2)} \geq \rho_{n-1}^{(2)}$ implies $\rho_{n+1}^{(2)} \geq \rho_n^{(2)}$. Therefore (5.6) implies

$$\rho_0^{(2)} > \dots > \rho_k^{(2)} > \rho_{k+1}^{(2)}. \quad (5.8)$$

According to matching conditions (3.6),

$$j^{(1)} = j_0^{(2)} + J^{(2)} - \rho_0^{(2)} R_1 = j_0^{(2)} + R_0(1 - R_1) - \rho_0^{(2)} R_1 = j_0^{(2)} + R_0 - \rho_{N_1}^{(1)} R_1, \quad (5.9)$$

and due to the relations $j_0^{(2)} = \rho_0^{(2)}(1 - \rho_1^{(2)}) > \rho_0^{(2)}(1 - \rho_0^{(2)})$ and $R_0 > R_1$,

$$j^{(1)} > \rho_0^{(2)}(1 - \rho_0^{(2)}) + R_0 - \rho_{N_1}^{(1)} R_0,$$

where $\rho_0^{(2)} = (1 - c)\rho_{N_1}^{(1)}$, $R_0 = c\rho_{N_1}^{(1)}$. Therefore,

$$j^{(1)} > (1 - c)\rho_{N_1}^{(1)}(1 - (1 - c)\rho_{N_1}^{(1)}) + c\rho_{N_1}^{(1)}(1 - \rho_{N_1}^{(1)}) = \rho_{N_1}^{(1)} - (c + (1 - c)^2)(\rho_{N_1}^{(1)})^2,$$

hence from $c < 1$ it follows that $j^{(1)} > \rho_{N_1}^{(1)}(1 - \rho_{N_1}^{(1)})$, which due to Lemma 5.1 implies $\rho_0^{(1)} > \dots > \rho_{N_1}^{(1)}$. Combining this with $\rho_0^{(2)} = c\rho_{N_1}^{(1)} < \rho_{N_1}^{(1)}$ and (5.8) proves (5.7). \square

5.2 Proof of Theorem 3.1

For a given $\rho_0^{(1)} = \rho^0$, take $j^{(1)} = \psi_{N_1}(\rho^0)$. Then, according to Lemma 5.1,

$$\rho_0^{(1)} > \rho_1^{(1)} > \dots > \rho_{N_1}^{(1)} = 0.$$

Lemma 5.1 further implies that given any $\varepsilon > 0$, we can find a $j^{(1)} \in (\frac{1}{2}\psi_{N_1}(\rho^0), \psi_{N_1}(\rho^0))$, such that sequence (3.3) satisfies

$$\rho^0 = \rho_0^{(1)} > \rho_1^{(1)} > \dots > \rho_{N_1}^{(1)} > 0; \quad \rho_{N_1}^{(1)} < \varepsilon. \quad (5.10)$$

Therefore, matching conditions (3.6) imply

$$\rho_0^{(2)} = (1 - c)\rho_{N_1}^{(1)} < \varepsilon, \quad J^{(2)} < R_0 = c\rho_{N_1}^{(1)} < \varepsilon$$

and

$$j_0^{(2)} = j^{(1)} - J^{(2)} + \rho_0^{(2)} R_1 > \frac{1}{2}\psi_{N_1}(\rho^0) - \varepsilon,$$

and from (3.3) it follows that

$$\rho_1^{(2)} < 1 - \frac{j_0^{(2)}}{\varepsilon}.$$

Therefore, for a sufficiently small ε , we obtain

$$\rho_0^{(2)} > 0 > \rho_1^{(2)}, \quad j_0^{(2)} > 0. \quad (5.11)$$

We now show by induction that if for some $k \geq 0$ and $A_k > 0$,

$$j^{(1)} = A_k \Rightarrow \rho_0^{(1)} > \dots > \rho_{N_1}^{(1)} > \rho_0^{(2)} > \dots > \rho_k^{(2)} > 0 > \rho_{k+1}^{(2)}; \quad j_k^{(2)} > 0, \quad (5.12)$$

then there is an $A_{k+1} \in (0, A_k)$ such that

$$j^{(1)} = A_{k+1} \Rightarrow \rho_0^{(1)} > \dots > \rho_{N_1}^{(1)} > \rho_0^{(2)} > \dots > \rho_{k+1}^{(2)} > 0 > \rho_{k+2}^{(2)}; \quad j_{k+1}^{(2)} > 0. \quad (5.13)$$

Relations (5.10), (5.11) establish the basis for the induction.

For the induction step, assume that (5.12) holds for a $k \geq 0$. Let us consider how the values $\rho_n^{(1)} = \rho_n^{(1)}(j^{(1)})$ and $\rho_n^{(2)} = \rho_n^{(2)}(j^{(1)})$ change when $j^{(1)}$ decreases from the value $j^{(1)} = A_k$. By Lemma 5.1, $\rho_{N_1}^{(1)}$ increases with decreasing $j^{(1)}$. Hence, $\rho_0^{(2)} = (1-c)\rho_{N_1}^{(1)}$, $R_0 = c\rho_{N_1}^{(1)}$ increase, and according to Remark 5.2, all $R_n = R_n(\psi_{N_2}(R_0), R_0)$ and all the differences $R_n - R_{n+2}$ with $n = 0, \dots, N_2 - 1$ also increase. Further, (5.9) implies that

$$j^{(1)} = j_0^{(2)} + (R_0 - R_1)\rho_{N_1}^{(1)} + (1 - \rho_{N_1}^{(1)})R_0 = j_0^{(2)} + (R_0 - R_1)\rho_{N_1}^{(1)} + c(1 - \rho_{N_1}^{(1)})\rho_{N_1}^{(1)},$$

where $R_0 - R_1$, $\rho_{N_1}^{(1)}$ and $(1 - \rho_{N_1}^{(1)})\rho_{N_1}^{(1)}$ increase with decreasing $j^{(1)}$ as long as $\rho_{N_1}^{(1)} < 1/2$, and hence $j_0^{(2)}$ decreases. Therefore, Lemma 5.2 implies that all $\rho_n^{(2)}$, $n = 0, \dots, k$ increase, and in particular $\rho_0^{(2)}, \dots, \rho_k^{(2)}$ remain positive, while all $j_n^{(2)}$, $n = 0, \dots, k$ decrease, as long as $j_k^{(2)}$ remains positive with decreasing $j^{(1)}$. Combining this with Lemma 5.3, we see that the ordering

$$1/2 \geq \rho_0^{(1)} > \dots > \rho_{N_1}^{(1)} > \rho_0^{(2)} > \dots > \rho_k^{(2)} > 0$$

is preserved, and all $\rho_0^{(1)}, \dots, \rho_{N_1}^{(1)}, \rho_0^{(2)}, \dots, \rho_k^{(2)}$ increase with decreasing $j^{(1)}$ as long as the relations $\rho_k^{(2)} > \rho_{k+1}^{(2)}$, $j_k^{(2)} > 0$ remain valid. Now, note that $j^{(1)} > j_0^{(2)} \geq \dots \geq j_k^{(2)}$ due to the second equation of (3.5) and (5.9). Hence, using the continuous dependence of $j_k^{(2)}$ on $j^{(1)}$, we conclude that there is a value $\tilde{A} \in [0, A_k)$ such that $j_k^{(2)} \rightarrow 0+$ as $j^{(1)} \rightarrow \tilde{A}+$. Further,

$$\rho_{k+1}^{(2)} = 1 - \frac{j_k^{(2)}}{\rho_k^{(2)}} \rightarrow 1 \quad \text{as} \quad j^{(1)} \rightarrow \tilde{A}+$$

because $\rho_k^{(2)}(\tilde{A}) > \rho_k^{(2)}(A_k) > 0$. Combining this with $\rho_{k+1}^{(2)}(A_k) < 0$, which is one of the induction assumptions, and using the continuity of $\rho_{k+1}^{(2)}(j^{(1)})$, we see that there is an $\hat{A} \in (\tilde{A}, A_k) \subset (0, A_k)$ such that $\rho_{k+1}^{(2)}(\hat{A}) = 0$ or, equivalently, $j_k^{(2)}(\hat{A}) = \rho_k^{(2)}(\hat{A})$. Hence,

$$j^{(1)} = \hat{A} \Rightarrow \rho_0^{(2)} > \dots > \rho_k^{(2)} > 0 = \rho_{k+1}^{(2)}; \quad j_k^{(2)} = \rho_k^{(2)} > 0; \quad j_{k+1}^{(2)} > 0, \quad (5.14)$$

where the last inequality follows from the relations $j_{k+1}^{(2)} = j_k^{(2)} - R_{k+1}\rho_k^{(2)} = (1 - R_{k+1})\rho_k^{(2)}$ in which $R_{k+1} \leq R_0 = c\rho_{N_1}^{(1)} \leq c < 1$. Again, using the continuity and monotonicity argument, relations (5.14) imply

$$\rho_{k+1}^{(2)} \rightarrow 0+, \quad \rho_{k+2}^{(2)} = 1 - \frac{j_{k+1}^{(2)}}{\rho_{k+1}^{(2)}} \rightarrow -\infty \quad \text{as} \quad j^{(1)} \rightarrow \hat{A}-. \quad (5.15)$$

Thus, relations (5.14), (5.15) and Lemma 5.3 imply (5.13) for $A_{k+1} = \hat{A} - \delta > 0$ with a sufficiently small $\delta > 0$, which completes the proof of the induction step.

Finally, the induction ensures the existence of a $j^{(1)} > 0$ for which $j_{N_2+N_3-1}^{(2)} > 0$, all $\rho_n^{(2)}$, $n = 0, \dots, N_2 + N_3 - 1$ are positive, and $\rho_{N_2+N_3}^{(2)} < 0$. Repeating the argument that was already used above in the proof of the induction step, one can now decrease $j^{(1)}$ to a smaller positive value to achieve $\rho_0^{(1)} > \dots > \rho_{N_1}^{(1)} > \rho_0^{(2)} > \dots > \rho_{N_2+N_3}^{(2)} = 0$. Relations $R_0 > \dots > R_{N_2} = 0$ follow from Lemma 5.1. This completes the proof of Theorem 3.1. \square

5.3 Proof of Theorem 3.2

Let (3.7) be a positive decreasing solution of problem (3.3)–(3.6) with $\rho^0 \in (0, 1/2)$. First, let us show that

$$j_m^{(2)} - \varphi(\rho_m^{(2)}) = O(N_2^{-1}), \quad 0 \leq m \leq N_2 + \frac{\ln N_2}{\ln q}. \quad (5.16)$$

Recall that $x_m = O(N_2^\alpha)$ is equivalent to $|x_m| \leq CN_2^\alpha$ where C is independent of N_2 for the given range m .

Using function (3.8), formula (3.4) can be rewritten as

$$\rho_{m+1}^{(2)} = \rho_m^{(2)} + \frac{\varphi(\rho_m^{(2)}) - j_m^{(2)}}{\rho_m^{(2)}}. \quad (5.17)$$

Introducing the notation

$$y_m = j_m^{(2)} - \varphi(\rho_m^{(2)}),$$

we see that

$$y_{m+1} - y_m = j_{m+1}^{(2)} - j_m^{(2)} + \varphi(\rho_m^{(2)}) - \varphi\left(\rho_m^{(2)} - \frac{y_m}{\rho_m^{(2)}}\right)$$

and using an intermediate value of the derivative of φ ,

$$y_{m+1} - y_m = j_{m+1}^{(2)} - j_m^{(2)} + \frac{y_m}{\rho_m^{(2)}} \varphi' \left(\rho_m^{(2)} - \frac{\theta_m y_m}{\rho_m^{(2)}} \right),$$

where $\theta_m \in [0, 1]$. Due to concavity of the function φ and relations $\rho_m^{(2)} < \rho^0 < 1/2$, we have

$$\frac{1}{\rho_m^{(2)}} \varphi' \left(\rho_m^{(2)} - \frac{\theta_m y_m}{\rho_m^{(2)}} \right) \geq \frac{\varphi'(\rho_m^{(2)})}{\rho_m^{(2)}} = \frac{1 - 2\rho_m^{(2)}}{\rho_m^{(2)}} > \frac{1}{\rho^0} - 2 > 0,$$

hence

$$y_{m+1} \geq j_{m+1}^{(2)} - j_m^{(2)} + \frac{y_m}{q}, \quad q := \frac{\rho^0}{1 - \rho^0} < 1.$$

Consequently,

$$y_m \leq q^{N_2 - m} y_{N_2} + \frac{q}{1 - q} \max_{0 \leq m \leq N_2} (j_m^{(2)} - j_{m+1}^{(2)}),$$

where $y_{N_2} = j_{N_2}^{(2)} - \varphi(\rho_{N_2}^{(2)}) \leq j_{N_2}^{(2)} \leq \rho_{N_2}^{(2)} < \rho^0$ and according to (3.5),

$$j_m^{(2)} - j_{m+1}^{(2)} = R_{m+1} \rho_m^{(2)} + (R_m - R_{m+2}) \rho_{m+1}^{(2)} \leq 2R_0 \rho_0^{(2)} = 2c(1 - c)(\rho_{N_1}^{(1)})^2 \leq \frac{2c_0(\rho^0)^2}{N_2}.$$

Therefore,

$$y_m \leq q^{N_2 - m} \rho^0 + \frac{2qc_0(\rho^0)^2}{(1 - q)N_2}.$$

In particular,

$$y_m \leq \frac{\rho^0}{N_2} \left(1 + \frac{2qc_0\rho^0}{1 - q} \right), \quad 0 \leq m \leq N_2 + \frac{\ln N_2}{\ln q},$$

where $y_m = j_m^{(2)} - \varphi(\rho_m^{(2)}) = \rho_m^{(2)}(1 - \rho_{m+1}^{(2)}) - \rho_m^{(2)}(1 - \rho_m^{(2)}) \geq 0$. This proves (5.16).

Next, we obtain estimates for the differences $R_m - R_{m+1} > 0$ and $R_0 - R_m > 0$. Relation (5.4) implies that

$$R_m - R_{m+1} = \frac{R_{N_2-1} - R_{N_2}}{\left(\frac{1}{R_0} - 1\right)^{N_2 - m - 1}} \leq R_0 \left(\frac{R_0}{1 - R_0}\right)^{N_2 - m - 1}.$$

Therefore,

$$R_0 - R_m \leq \frac{R_0}{1 - \frac{R_0}{1 - R_0}} \left(\frac{R_0}{1 - R_0}\right)^{N_2 - m}.$$

Since $R_0 = c\rho_{N_1}^{(1)} \leq c\rho^0 = c_0\rho^0/N_2$, it follows that

$$R_m - R_{m+1} = O(N_2^{m - N_2}), \quad R_0 - R_m = O(N_2^{m - N_2 - 1}). \quad (5.18)$$

Now, let us consider the initial value problem

$$\frac{d\hat{j}}{d\tau} = -c_0\rho^0\hat{\rho}(\tau), \quad \hat{j} = \varphi(\hat{\rho}) = \hat{\rho}(1 - \hat{\rho}); \quad \hat{j}(0) = \varphi(\rho_0^{(2)}) \quad (5.19)$$

on the interval $0 \leq \tau \leq 1$. Its solution is given by

$$\hat{j}(\tau) = \varphi(\hat{\rho}(\tau)), \quad \hat{\rho}(\tau) = -\frac{1}{2} W \left(-2\rho_0^{(2)} e^{-2\rho_0^{(2)} - c_0\rho^0\tau} \right). \quad (5.20)$$

Denote by φ^{-1} the inverse of the restriction $\varphi : [0, 1/2] \rightarrow \mathbb{R}_+$ of function (3.8) to its interval of monotonicity $[0, 1/2]$. Set

$$\hat{j}_m = \hat{j}(mh), \quad \hat{\rho}_m = \hat{\rho}(mh) = \varphi^{-1}(\hat{j}_m), \quad m = 0, 1, \dots, N_2; \quad h := 1/N_2.$$

Since $\hat{\rho}(\tau)$ decreases, (5.19) implies

$$\hat{j}_{m+1} - \hat{j}_m = -hc_0\rho^0(\chi_m\hat{\rho}_m + (1 - \chi_m)\hat{\rho}_{m+1}), \quad (5.21)$$

where $\chi_m \in [0, 1]$ for each $m = 0, \dots, N_2 - 1$. Let us estimate the error

$$e_m = j_m^{(2)} - \hat{j}_m.$$

Subtracting (5.21) from (3.5) gives

$$\begin{aligned} e_{m+1} - e_m &= -R_{m+1}\rho_m^{(2)} - (R_m - R_{m+2})\rho_{m+1}^{(2)} + hc_0\rho^0(\chi_m\hat{\rho}_m + (1 - \chi_m)\hat{\rho}_{m+1}) \\ &= (R_0 - R_{m+1})\rho_m^{(2)} - (R_m - R_{m+2})\rho_{m+1}^{(2)} + hc_0\rho^0(1 - \chi_m)(\hat{\rho}_{m+1} - \hat{\rho}_m) \\ &\quad + (hc_0\rho^0 - R_0)\rho_m^{(2)} + hc_0\rho^0(\hat{\rho}_m - \rho_m^{(2)}). \end{aligned}$$

Combining this with $h = 1/N_2$ and (5.18), we obtain

$$e_{m+1} - e_m = O(N_2^{m+1-N_2}) - hc_0\rho^0(1 - \chi_m)(\hat{\rho}_m - \hat{\rho}_{m+1}) + (hc_0\rho^0 - R_0)\rho_m^{(2)} + hc_0\rho^0(\hat{\rho}_m - \rho_m^{(2)}).$$

From

$$0 \leq \hat{\rho}_m - \hat{\rho}_{m+1} = -h \frac{d\hat{\rho}}{d\tau}(\tau_m) = \frac{-h}{1 - 2\hat{\rho}(\tau_m)} \cdot \frac{dj}{d\tau}(\tau_m) = h^2 c_0 \rho^0 \frac{\hat{\rho}(\tau_m)}{1 - 2\hat{\rho}(\tau_m)},$$

where $mh \leq \tau_m \leq (m+1)h$ and $\hat{\rho}(\tau_m) \leq \hat{\rho}_m \leq \hat{\rho}_0 = \rho_0^{(2)} \leq \rho^0$, it follows that

$$0 \leq \hat{\rho}_m - \hat{\rho}_{m+1} \leq \frac{h^2 c_0 (\rho^0)^2}{1 - 2\rho^0},$$

hence

$$e_{m+1} - e_m = O(N_2^{m+1-N_2}) + O(N_2^{-2}) + (hc_0\rho^0 - R_0)\rho_m^{(2)} + hc_0\rho^0(\hat{\rho}_m - \rho_m^{(2)}). \quad (5.22)$$

According to matching conditions (3.6),

$$j^{(1)} = j_0^{(2)} - \rho_0^{(2)}R_1 + J^{(2)} = j_0^{(2)} - \rho_0^{(2)}R_1 + R_0(1 - R_1),$$

which together with (5.16) implies

$$j^{(1)} = j_0^{(2)} + O(N_2^{-1}), \quad (5.23)$$

hence

$$j^{(1)} = \rho_0^{(1)}(1 - \rho_1^{(1)}) \geq \rho_0^{(1)}(1 - \rho_0^{(1)}) = \varphi(\rho^0) \geq \varphi(\rho_0^{(2)}) = j^{(1)} + O(N_2^{-1})$$

and therefore

$$\varphi(\rho^0) = j^{(1)} + O(N_2^{-1}), \quad \varphi(\rho_0^{(2)}) = j^{(1)} + O(N_2^{-1}). \quad (5.24)$$

Due to $0 < j^{(1)} < \rho^0 < 1/2$, from these relations and the relations

$$c_0\rho^0 - N_2R_0 = c_0(\rho^0 - \rho_{N_1}^{(1)}) = c_0 \left(\rho^0 - \frac{\rho_0^{(2)}}{1 - \frac{c_0}{N_2}} \right) = c_0(\rho^0 - \rho_0^{(2)}) + O(N_2^{-1}),$$

it follows that $c_0\rho^0 - N_2R_0 = O(N_2^{-1})$, and (5.22) implies

$$e_{m+1} - e_m = \frac{c_0\rho^0(\hat{\rho}_m - \rho_m^{(2)})}{N_2} + O(N_2^{-2})$$

for $m \leq N_2 - 3$. Combining this with $\hat{\rho}_m = \varphi^{-1}(\hat{j}_m)$ and (5.16) gives

$$e_{m+1} - e_m = c_0\rho^0 \frac{\varphi^{-1}(\hat{j}_m) - \varphi^{-1}(j_m^{(2)} + O(N_2^{-1}))}{N_2} + O(N_2^{-2})$$

for $0 \leq m \leq N_2 + \frac{\ln N_2}{\ln q}$, and due to

$$\frac{d\varphi^{-1}}{dj}(j) = \frac{1}{1 - 2\varphi^{-1}(j)}, \quad 0 < \hat{\rho}_m, \rho_m^{(2)} \leq \rho_0^{(2)} < \rho^0,$$

we obtain

$$|e_{m+1} - e_m| \leq \frac{c_0\rho^0|\hat{j}_m - j_m^{(2)}|}{(1 - 2\rho^0)N_2} + O(N_2^{-2}) = \frac{c_0\rho^0|e_m|}{(1 - 2\rho^0)N_2} + O(N_2^{-2}).$$

By discrete Grönwall's inequality, this implies

$$|e_m| \leq e^{\frac{\kappa m}{N_2}} |e_0| + \frac{N_2(e^{\frac{\kappa m}{N_2}} - 1)}{\kappa} \cdot O(N_2^{-2}) = e^{\frac{\kappa m}{N_2}} |e_0| + O(N_2^{-1}), \quad \kappa := \frac{c_0\rho^0}{1 - 2\rho^0},$$

with $e_0 = j_0^{(2)} - \hat{j}_0 = j_0^{(2)} - \varphi(\rho_0^{(2)}) = O(N_2^{-1})$, where the last equality follows from (5.16), hence

$$e_m = O(N_2^{-1}) \quad \text{for all } 0 \leq m \leq N_2 + \frac{\ln N_2}{\ln q}. \quad (5.25)$$

Finally, relations (3.5) and (5.19) ensure that $j_m^{(2)} - j_{m+1}^{(2)} = O(N_2^{-1})$ and $\hat{j}_m - \hat{j}_{m+1} = O(N_2^{-1})$, hence

$$e_m = O(N_2^{-1} \ln N_2) \quad \text{for all } 0 \leq m \leq N_2 \quad (5.26)$$

Combining (5.25), (5.26) with relations (5.16), (5.20), (5.23), (5.24) and $\rho^0 = \rho_0^{(1)} > \dots > \rho_{N_1}^{(1)} > \rho_0^{(2)}$, we obtain (3.10)–(3.14). This completes the proof.

6. Conclusion

We proposed a deterministic model for the translation of an uORF with leaky scanning initiation. The model assumes that the collision of elongating and scanning ribosomes can result in detachment of the latter from the mRNA. We showed that the dependence of the flow of scanning ribosomes downstream of the uORF on the density of scanning ribosomes upstream of the uORF for the stationary solution is non-monotone provided that the uORF is sufficiently long and the fraction of the initiated ribosomes is sufficiently small. In particular, reducing the ribosome flow upstream of the uORF can increase the flow downstream. Further, we obtained an explicit formula for the flow downstream of the uORF in the limit when the length N of the uORF increases and the initiation efficiency decreases as $1/N$ (see (3.8), (3.9) and (3.14)). These analytical results agree with earlier numerical findings obtained by TASEP modeling

under similar assumptions (Andreev *et al.*, 2018). We showed numerically that the downstream flow predicted by the deterministic model and the TASEP model can be relatively close to our analytical solution for realistic values of N . Therefore, our model provides a plausible explanation for the experimentally confirmed ability of a single uORF to upregulate the downstream ORF translation when the upstream flow of ribosomes is reduced due to stress. We associate the mechanism of upregulation with the above stated assumption that some scanning ribosomes dissociate from the uORF before reaching the stop codon as a result of interaction with the elongating ribosomes. Our results predict that stress resistance can be achieved by translation of relatively long uORFs that do not favor high levels of translation initiation. In general these findings are relevant not only to IRS, but to any changes in intracellular conditions that affect the flow of scanning ribosomes or parameters of uORF translation, e.g., induction of a ribosome pause at uORF or uORF initiation rate.

Acknowledgments

The authors thank M. Arnold for useful discussion of the models and results. This work was supported by Russian Science Foundation (20-14-00121).

REFERENCES

- HINNEBUSCH, A.G., IVANOV, I.P. AND SONENBERG, N. (2016) Translational control by 5'-untranslated regions of eukaryotic mRNAs. *Science*, **352**, 1413-1416.
- HINNEBUSCH, A.G. (2014) The scanning mechanism of eukaryotic translation initiation. *Annu Rev Biochem*, **83**, 779-812.
- ASANO, K. (2014) Why is start codon selection so precise in eukaryotes? *Translation (Austin)*, **2**, e28387.
- TOPISIROVIC, I., SVITKIN, Y.V., SONENBERG, N. AND SHATKIN, A.J. (2011) Cap and cap-binding proteins in the control of gene expression. *Wiley Interdiscip Rev RNA*, **2**, 277-298.
- JACKSON, R.J., HELLEN, C.U. AND PESTOVA, T.V. (2010) The mechanism of eukaryotic translation initiation and principles of its regulation. *Nat Rev Mol Cell Biol*, **11**, 113-127.
- PUEYO, J.I., MAGNY, E.G. AND COUSO, J.P. (2016) New Peptides Under the s(ORF)ace of the Genome. *Trends Biochem Sci*, **41**, 665-678.
- JOHNSTONE, T.G., BAZZINI, A.A. AND GIRALDEZ, A.J. (2016) Upstream ORFs are prevalent translational repressors in vertebrates. *EMBO J*, **35**, 706-723.
- WETHMAR, K. (2014) The regulatory potential of upstream open reading frames in eukaryotic gene expression. *Wiley Interdiscip Rev RNA*, **5**, 765-778.
- VON ARNIM, A.G., JIA, Q. AND VAUGHN, J.N. (2014) Regulation of plant translation by upstream open reading frames. *Plant Sci*, **214**, 1-12.
- BARBOSA, C., PEIXEIRO, I. AND ROMAO, L. (2013) Gene expression regulation by upstream open reading frames and human disease. *PLoS Genet*, **9**, e1003529.
- SOMERS, J., POYRY, T. AND WILLIS, A.E. (2013) A perspective on mammalian upstream open reading frame function. *Int J Biochem Cell Biol*, **45**, 1690-1700.
- VILELA, C. AND MCCARTHY, J.E. (2003) Regulation of fungal gene expression via short open reading frames in the mRNA 5'-untranslated region. *Mol Microbiol*, **49**, 859-867.
- CHURBANOV, A., ROGOZIN, I.B., BABENKO, V.N., ALI, H. AND KOONIN, E.V. (2005) Evolutionary conservation suggests a regulatory function of AUG triplets in 5'-UTRs of eukaryotic genes. *Nucleic Acids Res*, **33**, 5512-5520.
- IVANOV, I.P., FIRTH, A.E., MICHEL, A.M., ATKINS, J.F. AND BARANOV, P.V. (2011) Identification of evolutionarily conserved non-AUG-initiated N-terminal extensions in human coding sequences. *Nucleic Acids Res*,

- 39**, 4220-4234.
- IVANOV, I.P., LOUGHRAN, G. AND ATKINS, J.F. (2008) uORFs with unusual translational start codons autoregulate expression of eukaryotic ornithine decarboxylase homologs. *Proc Natl Acad Sci U S A*, **105**, 10079-10084.
- PEABODY, D.S. (1989) Translation initiation at non-AUG triplets in mammalian cells. *J Biol Chem*, **264**, 5031-5035.
- TZANI, I., IVANOV, I.P., ANDREEV, D.E., DMITRIEV, R.I., DEAN, K.A., BARANOV, P.V., ATKINS, J.F. AND LOUGHRAN, G. (2016) Systematic analysis of the PTEN 5' leader identifies a major AUU initiated proteoform. *Open Biol*, **6**.
- MICHEL, A.M., ANDREEV, D.E. AND BARANOV, P.V. (2014) Computational approach for calculating the probability of eukaryotic translation initiation from ribo-seq data that takes into account leaky scanning. *BMC Bioinformatics*, **15**, 380.
- FRITSCH, C., HERRMANN, A., NOTHNAGEL, M., SZAFRANSKI, K., HUSE, K., SCHUMANN, F., SCHREIBER, S., PLATZER, M., KRAWCZAK, M., HAMPE, J. ET AL. (2012) Genome-wide search for novel human uORFs and N-terminal protein extensions using ribosomal footprinting. *Genome Res*, **22**, 2208-2218.
- INGOLIA, N.T., LAREAU, L.F. AND WEISSMAN, J.S. (2011) Ribosome profiling of mouse embryonic stem cells reveals the complexity and dynamics of mammalian proteomes. *Cell*, **147**, 789-802.
- LEE, S., LIU, B., LEE, S., HUANG, S.X., SHEN, B. AND QIAN, S.B. (2012) Global mapping of translation initiation sites in mammalian cells at single-nucleotide resolution. *Proc Natl Acad Sci U S A*, **109**, E2424-2432.
- ANDREEV, D.E., O'CONNOR, P.B., ZHDANOV, A.V., DMITRIEV, R.I., SHATSKY, I.N., PAPKOVSKY, D.B. AND BARANOV, P.V. (2015) Oxygen and glucose deprivation induces widespread alterations in mRNA translation within 20 minutes. *Genome Biol*, **16**, 90.
- SHALGI, R., HURT, J.A., KRYKBAEVA, I., TAIPALE, M., LINDQUIST, S. AND BURGE, C.B. (2013) Widespread regulation of translation by elongation pausing in heat shock. *Mol Cell*, **49**, 439-452.
- GERASHCHENKO, M.V., LOBANOV, A.V. AND GLADYSHEV, V.N. (2012) Genome-wide ribosome profiling reveals complex translational regulation in response to oxidative stress. *Proc Natl Acad Sci U S A*, **109**, 17394-17399.
- INGOLIA, N.T., GHAEMMAGHAMI, S., NEWMAN, J.R. AND WEISSMAN, J.S. (2009) Genome-wide analysis in vivo of translation with nucleotide resolution using ribosome profiling. *Science*, **324**, 218-223.
- ANDREEV, D.E., O'CONNOR, P.B., FAHEY, C., KENNY, E.M., TERENCE, I.M., DMITRIEV, S.E., CORMICAN, P., MORRIS, D.W., SHATSKY, I.N. AND BARANOV, P.V. (2015) Translation of 5' leaders is pervasive in genes resistant to eIF2 repression. *Elife*, **4**, e03971.
- STARCK, S.R., TSAI, J.C., CHEN, K., SHODIYA, M., WANG, L., YAHIRO, K., MARTINS-GREEN, M., SHASTRI, N. AND WALTER, P. (2016) Translation from the 5' untranslated region shapes the integrated stress response. *Science*, **351**, aad3867.
- YOUNG, S.K. AND WEK, R.C. (2016) Upstream Open Reading Frames Differentially Regulate Gene-specific Translation in the Integrated Stress Response. *J Biol Chem*, **291**, 16927-16935.
- BAIRD, T.D. AND WEK, R.C. (2012) Eukaryotic initiation factor 2 phosphorylation and translational control in metabolism. *Adv Nutr*, **3**, 307-321.
- SIDRAUSKI, C., MCGEACHY, A.M., INGOLIA, N.T. AND WALTER, P. (2015) The small molecule ISRIB reverses the effects of eIF2alpha phosphorylation on translation and stress granule assembly. *Elife*, **4**.
- HINNEBUSCH, A.G. (1993) Gene-specific translational control of the yeast GCN4 gene by phosphorylation of eukaryotic initiation factor 2. *Mol Microbiol*, **10**, 215-223.
- GUNISOVA, S., BEZOSKOVA, P., MOHAMMAD, M.P., VLCKOVA, V. AND VALASEK, L.S. (2016) In-depth analysis of cis-determinants that either promote or inhibit reinitiation on GCN4 mRNA after translation of its four short uORFs. *RNA*, **22**, 542-558.
- GUNISOVA, S. AND VALASEK, L.S. (2014) Fail-safe mechanism of GCN4 translational control—uORF2 promotes reinitiation by analogous mechanism to uORF1 and thus secures its key role in GCN4 expression. *Nucleic*

- Acids Res*, **42**, 5880-5893.
- DEVER, T.E., FENG, L., WEK, R.C., CIGAN, A.M., DONAHUE, T.F. AND HINNEBUSCH, A.G. (1992) Phosphorylation of initiation factor 2 alpha by protein kinase GCN2 mediates gene-specific translational control of GCN4 in yeast. *Cell*, **68**, 585-596.
- PALAM, L.R., BAIRD, T.D. AND WEK, R.C. (2011) Phosphorylation of eIF2 facilitates ribosomal bypass of an inhibitory upstream ORF to enhance CHOP translation. *J Biol Chem*, **286**, 10939-10949.
- CHEN, Y.J., TAN, B.C., CHENG, Y.Y., CHEN, J.S. AND LEE, S.C. (2010) Differential regulation of CHOP translation by phosphorylated eIF4E under stress conditions. *Nucleic Acids Res*, **38**, 764-777.
- LEE, Y.Y., CEVALLOS, R.C. AND JAN, E. (2009) An upstream open reading frame regulates translation of GADD34 during cellular stresses that induce eIF2alpha phosphorylation. *J Biol Chem*, **284**, 6661-6673.
- ZACH, L., BRAUNSTEIN, I. AND STANHILL, A. (2014) Stress-induced start codon fidelity regulates arsenite-inducible regulatory particle-associated protein (AIRAP) translation. *J Biol Chem*, **289**, 20706-20716.
- YOUNG, S.K., PALAM, L.R., WU, C., SACHS, M.S. AND WEK, R.C. (2016) Ribosome Elongation Stall Directs Gene-specific Translation in the Integrated Stress Response. *J Biol Chem*, **291**, 6546-6558.
- ANDREEV D.E., ARNOLD M., KINIRY S.J., LOUGHRAN G., MICHEL A.M., RACHINSKII D., BARANOV P.V. (2018) TASEP modelling provides a parsimonious explanation for the ability of a single uORF to derepress translation during the integrated stress response. *Elife*, **7**:e32563
- MACDONALD, C. T., GIBBS, J. H., AND PIPKIN, A. C. (1968) Kinetics of biopolymerization on nucleic acid templates. *Biopolymers*, **6(1)**, 1-25.
- CIANDRINI, L., STANSFIELD, I. AND ROMANO, M.C. (2010) Role of the particle's stepping cycle in an asymmetric exclusion process: a model of mRNA translation. *Phys Rev E Stat Nonlin Soft Matter Phys*, **81**, 051904.
- L. GRÜNE, T. KRIECHERBAUER, M. MARGALOT (2020) Random attraction in the TASEP model. *arXiv e-prints*, [arXiv:2001.07764](https://arxiv.org/abs/2001.07764).
- REUVENI, S., MEILIJSON, I., KUPIEC, M., RUPPIN, E. AND TULLER, T. (2011) Genome-scale analysis of translation elongation with a ribosome flow model. *PLoS Comput Biol*, **7**, e1002127.
- VON DER HAAR, T. (2012) Mathematical and Computational Modelling of Ribosomal Movement and Protein Synthesis: an overview. *Comput Struct Biotechnol J*, **1**, e201204002.
- ZHAO, Y.B. AND KRISHNAN, J. (2014) mRNA translation and protein synthesis: an analysis of different modelling methodologies and a new PBN based approach. *BMC Syst Biol*, **8**, 25.
- ZIA, R.K.P., DONG, J.J. AND SCHMITTMANN, B. (2011) Modeling translation in protein synthesis with TASEP: A tutorial and recent developments. *J Stat Phys*, **144**, 405.
- ZUR, H. AND TULLER, T. (2016) Predictive biophysical modeling and understanding of the dynamics of mRNA translation and its evolution. *Nucleic Acids Research*, **44(19)**, 9031-9049.
- A. N. GORBAN, A. HAREL-BELLAN, N. MOROZOVA, A. ZINOVYEV (2019) Basic, simple and extendable kinetic model of protein synthesis. *Mathematical Biosciences and Engineering*, **16(6)**, 6602-6622.
- DERRIDA, B., LEBOWITZ, J., AND SPEER, E. (1997) Shock profiles for the asymmetric simple exclusion process in one dimension. *Journal of Statistical Physics*, **89(1-2)**, 135-167.
- BLYTHE, R. A. AND EVANS, M. R. (2007). Nonequilibrium steady states of matrix-product form: a solver's guide. *Journal of Physics A: Mathematical and Theoretical*, **40(46)**, R333-R441.
- SCHÖNHERR, G. AND SCHÜTZ, G. (2004) Exclusion process for particles of arbitrary extension: hydrodynamic limit and algebraic properties. *Journal of Physics A: Mathematical and General*, **37(34)**, 8215-8231.
- ERDMANN-PHAM, D. D., DUC, K. D. AND SONG, YU. S. (2020) The key parameters that govern translation efficiency. *Cell Systems*, **10(2)**, 183-192.